Hindawi
Complexity
Volume 2022, Article ID 6122921, 11 pages
https://doi.org/10.1155/2022/6122921

Research Article

Event-Based State Estimation for Networked Singularly Perturbed Complex Networks

Zerong Ren

School of Mathematics, Zunyi Normal College, Zunyi 563006, China

Correspondence should be addressed to Zerong Ren; zerongren@163.com

Received 2 March 2022; Revised 22 June 2022; Accepted 27 June 2022; Published 14 July 2022

Academic Editor: Yue Song

Copyright © 2022 Zerong Ren. This is an open access article distributed under the Creative Commons Attribution License, which permits unrestricted use, distribution, and reproduction in any medium, provided the original work is properly cited.

This paper deals with the multievent-triggering-based state estimation for a class of discrete-time networked singularly perturbed complex networks (SPCNs). A small singularly perturbed scalar is adopted to establish a discrete-time SPCNs model. To reduce the communication burdens, the data transmission between the sensor and the estimator is managed by a multievent generator function. Depending on the singularly-perturbed-based Lyapunov theory, a sufficient condition is constructed to guarantee that the estimation error is exponentially ultimately bounded in the mean square. Finally, the validity of the developed result is demonstrated by a simulation example.

1. Introduction

A complex network is a set of interconnected nodes coupled by certain network topology, each node of which can be considered as a class of dynamic subsystems. Owing to its complex inherent structure, most systems in real life can be regarded simply as complex networks, including, but not limited to social networks, biological networks, power grid networks, and Internet [1–3]. Consequently, considerable research interest has been stirred over the past few decades and there has been a host of meaningful published achievements of complex networks [4–9].

As far as we know, however, the complex networks with two-time scales receive little attention. However, the two-time scale case of many real-life complex networks [10–12] is continually encountered. For instance, the circuit state variables become faster than the mechanical state variables in electronic power grids, due to the difference in the time scalars on the circuit and the mechanical systems [10]. This can result in the appearance of diverse time-scale subsystems in hosts of electromechanical systems, named fast and slow dynamics. In most of the existing literature [13–15], a singularly perturbed approach is adopted to deal with the two-time scale phenomenon of these real-life systems. In other words, the fast-slow subsystem is distinguished by introducing a small singularly perturbed scalar. Hence, such complex networks can be regarded as SPCNs [16–23].

What is worth mentioning is that a host of the reporting efforts [16–20] merely focuses on the synchronization phenomenon of the SPCNs. However, in some real-world scenarios, the exact state of the SPCNs on account of various factors, like the high number of nodes, disturbances in all directions, and high dimensions, is unavailable [7]. Thus, what we should pay attention to is the state estimation of the SPCNs. On the other hand, we noticed that besides [22, 23], the discrete-time SPCNs get little research concerns. The two important reasons for considering the discrete-time SPCNs are that computational simulation and network communication. Therefore, it is very necessary to investigate the state estimation of the discrete-time SPCNs.

In addition, increasing attention is devoted to the event-triggered protocol (ETP), in which the current packet is released if the ETP-based triggering condition is satisfied [24–26]. Past years have witnessed an increasing interest in ETPs, including static ETPs, dynamic ETPs, and memory ETPs [27–34]. It is noted that in the above-referred ETPs, the triggering parameter is assumed to be the same for all dynamic outputs/states. Nevertheless, such an assumption is difficult to be satisfied, especially in multisensor networks, which contributes to the varying triggering parameters. In light of above-discussed phenomenon, in this work, in order to save resource consumption and solve the communication congestion, a multi-ETP is employed to deal with the large information communication among nodes of the discrete-time SPCNs, which, to some extent, promotes the current research. As such, a natural and interesting question is how to design a proper multi-ETP for discrete-time SPCNs.

Based on the aforementioned observations, we try our best to develop the multi-ETP-based estimator design issue for the discrete-time SPCNs. Then, the mean square exponential bounded and state estimations are studied by using the Lyapunov function dependent on a singular perturbed parameter. In the end, a numerical example is presented to prove the effectiveness of the state estimator design method. It is worth emphasizing that even though the discrete-time SPCNs are unstable, the result of this work is still efficient. The highlights of our contributions are outlined as follows: (1) A nonlinear discrete-time SPCNs model is developed, which includes nonlinearities of complex networks and multitime scales. (2) As the study progress, the multi-ETP-based state estimation problem for the discrete-time SPCNs with nonlinearities is considered.

Notation: $\mathbb{N}$ refers to a set of all nonnegative integers. $\mathcal{Z}^\top$ represents the transpose of the matrix $\mathcal{Z}$. diag$\{\cdot\}$ symbolizes the diagonal matrix. $\mathbf{He}\{\mathcal{Z}\} = \mathcal{Z}^\top + \mathcal{Z}$. I_m denotes the m-dimensional unit matrix. $\lambda_{\min}(\cdot)/\lambda_{\max}(\cdot)$ denotes the minimal/maximal eigenvalue. $\|\cdot\|$ means Euclidean vector norm. $\mathscr{E}\{\cdot\}$ signifies the mathematical expectation.

2. Problem Formulations

Consider a type of SPCNs composed of N coupled nodes described by

$$\begin{cases} x_i(k+1) = g_\epsilon(x_i(k)) + \sum_{j=1}^{N} \omega_{ij}\Gamma_\epsilon x_j(k) + C_{i,\epsilon}\nu(k), \\ y_i(k) = D_i x_i(k) + E_i \nu(k), \ (i = 1, 2, \ldots, N), \end{cases} \tag{1}$$

where $x_i(k) = [x_{is}^\top(k) x_{if}^\top(k)]^\top \in \mathbb{R}^{n_x}$, $y_i(k) = [y_{is}^\top(k) y_{if}^\top(k)]^\top \in \mathbb{R}^{n_y}$, $g_\epsilon(x_i(k)) = \begin{bmatrix} f(x_{is}(k)) + Ax_{if}(k) \\ \epsilon(h(x_{is}(k)) + Bx_{if}(k)) \end{bmatrix}$, $\Gamma_\epsilon = \begin{bmatrix} \Gamma_{11} & \Gamma_{12} \\ \epsilon\Gamma_{21} & \epsilon\Gamma_{22} \end{bmatrix}$, $C_{i,\epsilon} = \begin{bmatrix} C_{is} \\ \epsilon C_{if} \end{bmatrix}$, $D_i = \text{diag}\{D_{is}, D_{if}\}$, $E_i = \begin{bmatrix} E_{is} \\ E_{if} \end{bmatrix}$, $x_{is}(k) \in \mathbb{R}^{n_{x_s}}$, and $x_{if}(k) \in \mathbb{R}^{n_{x_f}}$ ($n_x = n_{x_s} + n_{x_f}$) refer to the slow state and the fast state of node i, respectively. $y_{is}(k) \in \mathbb{R}^{n_{y_s}}$ and $y_{if}(k) \in \mathbb{R}^{n_{y_f}}$ ($n_y = n_{y_s} + n_{y_f}$) mean the measurement outputs of node i, ϵ is a singular perturbation parameter, and $\nu(k) \in \mathbb{R}^{n_\nu}$ signifies the bound disturbance input belonging to $l_2[0,\infty)$, which meets $\|\nu(k)\|^2 \le \bar{\nu}$. Γ_ϵ refers to an inner-coupling matrix with given dimensions. A, B, $C_{i,\epsilon}$, D_i, and E_i are known matrices with suitable dimensions.

The network topology $\mathfrak{W} = \{\mathcal{N}, \mathcal{X}, \mathcal{W}\}$ is devoted to reflect the outer coupling phenomenon of the SPCNs. $\mathcal{N} = \{1, 2, \ldots, N\}$ and $\mathcal{X} \subseteq \mathcal{N} \times \mathcal{N}$ symbolize the sets of nodes and edges. For any $(i, j \in \mathcal{N})$, the out-coupled configuration matrix $\mathcal{W} = \{\omega_{ij}\}$ is symmetric if $\omega_{ij} = \omega_{ji} > 0$, which satisfies

$$\omega_{ii} = -\sum_{j=1, j\neq i}^{N} \omega_{ij}, \tag{2}$$

where $\omega_{ij} > 0\, (\forall i \neq j)$ implies a connection between nodes j and i; otherwise, $\omega_{ij} = 0$.

Assumption 1 (see [23]). The nonlinear sector-valued functions $f(\cdot)\colon \mathbb{R}^{n_{x_s}} \longrightarrow \mathbb{R}^{n_{x_s}}$ and $h(\cdot)\colon \mathbb{R}^{n_{x_s}} \longrightarrow \mathbb{R}^{n_{x_f}}$ of SPCNs (1) satisfy the following assumption:

$$\begin{aligned} &\left[f(x_{is}(k)) - f(x_{js}(k)) - \Lambda_1(x_{is}(k) - x_{js}(k))\right]^\top \left[f(x_{is}(k)) - f(x_{js}(k)) - \Lambda_2(x_{is}(k) - x_{js}(k))\right] \le 0, \\ &\left[h(x_{is}(k)) - h(x_{js}(k)) - \Upsilon_1(x_{is}(k) - x_{js}(k))\right]^\top \left[h(x_{is}(k)) - h(x_{js}(k)) - \Upsilon_2(x_{is}(k) - x_{js}(k))\right] \le 0, \end{aligned} \tag{3}$$

where $x_{is}(k)$, $x_{js}(k) \in \mathbb{R}^{n_{x_s}}$, $f(0) = 0$, $h(0) = 0$, Λ_ℓ, and $\Upsilon_\ell\,(\ell = 1, 2)$ are constant matrices.

In this paper, for the sake of saving the communication resources between the sensors and estimators, a multievent-triggered approach is presented to reduce transmission energy. The triggering instant series of node i can be assumed as $0 \le k_0^i < k_1^i < \ldots < k_t^i < \ldots$, $(i = 1, 2, \ldots, N)$ where the new transmitted instant k_{t+1}^i can be formulated as

$$k_{t+1}^i = \min\left\{k \in [0, \mathbb{N}] | k > k_t^i, \theta_i - \varepsilon_i^\top(k)\Phi_i\varepsilon_i(k) < 0\right\}. \tag{4}$$

With $k_0^i = 0$, $\theta_i \in [0,1]$ is the given parameter of the i-th node, $\Phi_i = \text{diag}\{\Phi_{is}, \Phi_{if}\} > 0$ is a weighting matrix of the i-th node to be determined, and $\varepsilon_i(k) \triangleq y_i(k) - y_i(k_t^i) \triangleq [\varepsilon_{is}^\top(k)\varepsilon_{if}^\top(k)]^\top$ with $y_i(k_t^i)$ referring to the latest transmitted measurement of node i. Hence, for $k \in [k_t^i, k_{t+1}^i)$,

$$\theta_i - \varepsilon_i^\top(k)\Phi_i\varepsilon_i(k) \ge 0. \tag{5}$$

Remark 1. Note that different from the existing static ETP, the multievent-triggered protocol is studied in (2). The proposed triggering protocol can be seen as a generalized framework of ETP, which cover the existing static ETP as a special case (i.e., $i = 1$).

Subsequently, based on the multievent-triggered approach, a state estimator is constructed as

$$\hat{x}_i(k+1) = g_\epsilon(\hat{x}_i(k)) + \sum_{j=1}^{N} \omega_{ij}\Gamma_\epsilon \hat{x}_j(k) + K_i\left(y_i\left(k_t^i\right) - D_i\hat{x}_i(k)\right), (i = 1, 2, \ldots, N), \tag{6}$$

where $\hat{x}_i(k) = [\hat{x}_{is}^\top(k)\hat{x}_{if}^\top(k)]^\top$ with $\hat{x}_{is}(k)$ and $\hat{x}_{if}(k)$ representing the state estimations of $x_{is}(k)$ and $x_{if}(k)$, respectively. $K_i = \text{diag}\{K_{is}, K_{if}\}$ means the estimator gain of the i-th node to be judged.

Let

$$\begin{aligned}
\tilde{e}_i(k) &= \left[\tilde{e}_{is}^\top(k)\tilde{e}_{if}^\top(k)\right]^\top, \\
\tilde{e}_{is}(k) &= x_{is}(k) - \hat{x}_{is}(k), \\
\tilde{e}_{if}(k) &= x_{if}(k) - \hat{x}_{if}(k), \\
\mathfrak{A}(k) &= \left[\mathfrak{A}_1^\top(k)\mathfrak{A}_2^\top(k)\ldots\mathfrak{A}_N^\top(k)\right]^\top(\tilde{e}, \varepsilon,), \\
\tilde{\mathfrak{B}}(\tilde{e}_{is}(k)) &= \mathfrak{B}(x_{is}(k)) - \mathfrak{B}(\hat{x}_{is}(k))\,(\mathfrak{B} = f, h), \\
\tilde{g}_\epsilon^\top(\tilde{e}_{is}(k)) &= \left[\tilde{f}^\top(\tilde{e}_{is}(k))\epsilon\tilde{h}^\top(\tilde{e}_{is}(k))\right], \\
\vec{g}_\epsilon(\tilde{e}_s(k)) &= \left[\tilde{g}_\epsilon^\top(\tilde{e}_{1s}(k))\tilde{g}_\epsilon^\top(\tilde{e}_{2s}(k))\ldots\tilde{g}_\epsilon^\top(\tilde{e}_{Ns}(k))\right]^\top.
\end{aligned} \tag{7}$$

Combining (1) and (4), the dynamics of the estimation error can be built as

$$\tilde{e}(k+1) = \vec{g}_\epsilon(\tilde{e}_s(k)) + (\mathscr{W}\otimes\Gamma_\epsilon + I_N\otimes G_\epsilon - KD)\tilde{e}(k) + (C_\epsilon - KE)\nu(k) + K\varepsilon(k), \tag{8}$$

where

$$\begin{aligned}
C_\epsilon &= \left[C_{1,\epsilon}^\top C_{2,\epsilon}^\top\ldots C_{N,\epsilon}^\top\right]^\top, \\
\mathfrak{K} &= \text{diag}\{\mathfrak{K}_1, \mathfrak{K}_2, \ldots, \mathfrak{K}_N\}\,(\mathfrak{K} = K, D), \\
E &= \left[E_1^\top E_2^\top\ldots E_N^\top\right]^\top, \\
G_\epsilon &= \begin{bmatrix} 0 & A \\ 0 & \epsilon B \end{bmatrix}.
\end{aligned} \tag{9}$$

In the sequel, one reschedules the order of dynamic estimation errors (8). Denote $\mathscr{T} = \mathscr{T}_1\times\mathscr{T}_2\times\cdots\times\mathscr{T}_N$, with $\mathscr{T}_\ell\in\mathbb{R}^{Nn_x\otimes Nn_x}\,(\ell = 1, 2, \ldots, N)$ being row-switching elementary matrices and $\mathscr{T}$ being invertible. Then, one has

$$\mathscr{T}\tilde{e}(k+1) = \mathscr{T}\vec{g}_\epsilon(\tilde{e}_s(k)) + \mathscr{T}(\mathscr{W}\otimes\Gamma_\epsilon + I_N\otimes G_\epsilon - KD)\mathscr{T}^{-1}\mathscr{T}\tilde{e}(k) + \mathscr{T}(C_\epsilon - KE)\nu(k) + \mathscr{T}K\varepsilon(k), \tag{10}$$

which yields

$$e(k+1) = \mathscr{A}_\epsilon e(k) + \mathscr{I}_1\mathbf{f}(e_s(k)) + \epsilon\mathscr{I}_2\mathbf{h}(e_s(k)) + \mathscr{C}_\epsilon\nu(k) + \mathscr{K}\bar{\varepsilon}(k), \tag{11}$$

where

$$
\begin{aligned}
e(k) &= \left[\tilde{e}_{1s}^{\top}(k)\tilde{e}_{2s}^{\top}(k)\ldots\tilde{e}_{Ns}^{\top}(k)\tilde{e}_{1f}^{\top}(k)\tilde{e}_{2f}^{\top}(k)\ldots\tilde{e}_{Nf}^{\top}(k)\right]^{\top},\\
\mathfrak{D}(e_s(k)) &= \left[\tilde{\mathfrak{D}}^{\top}(\tilde{e}_{1s}(k))\tilde{\mathfrak{D}}^{\top}(\tilde{e}_{2s}(k))\ldots\tilde{\mathfrak{D}}^{\top}(\tilde{e}_{Ns}(k))\right]^{\top}(\mathfrak{D}=f,h),\\
\bar{\varepsilon}(k) &= \left[\varepsilon_{1s}^{\top}(k)\varepsilon_{2s}^{\top}(k)\ldots\varepsilon_{Ns}^{\top}(k)\varepsilon_{1f}^{\top}(k)\varepsilon_{2f}^{\top}(k)\ldots\varepsilon_{Nf}^{\top}(k)\right]^{\top},\\
\mathscr{A}_{\epsilon} &= \begin{bmatrix} -K_sD_s+\mathscr{W}\otimes\Gamma_{11} & I_N\otimes A+\mathscr{W}\otimes\Gamma_{12}\\ \epsilon(\mathscr{W}\otimes\Gamma_{21}) & \epsilon(I_N\otimes B+\mathscr{W}\otimes\Gamma_{22})-K_fD_f\end{bmatrix},\\
\mathscr{I}_1 &= \begin{bmatrix} I_{Nn_{x_s}}\\ 0_{Nn_{x_f}\times Nn_{x_s}}\end{bmatrix},\\
\mathscr{I}_2 &= \begin{bmatrix} 0_{Nn_{x_s}\times Nn_{x_f}}\\ I_{Nn_{x_f}}\end{bmatrix},\\
\mathscr{C}_{\epsilon} &= \begin{bmatrix} C_s-K_sE_s\\ \epsilon C_f-K_fE_f\end{bmatrix},\\
\mathscr{K} &= \operatorname{diag}\{K_s,K_f\},\\
\mathfrak{E}_{\ell} &= \operatorname{diag}\{\mathfrak{E}_{1\ell},\mathfrak{E}_{2\ell},\ldots,\mathfrak{E}_{N\ell}\}\,(\mathfrak{E}=K,D,\ell=s,f),\\
\mathfrak{F}_{\ell} &= \left[\mathfrak{F}_{1\ell}^{\top}\mathfrak{F}_{2\ell}^{\top}\ldots\mathfrak{F}_{N\ell}^{\top}\right]^{\top}(\mathfrak{F}=C,E,\ell=s,f).
\end{aligned}
\tag{12}
$$

To facilitate the derivation of the main results, the following definition and lemma are introduced.

Definition 1 (see [35]). Estimation error dynamics (7) is exponentially ultimately bounded in mean square (EUBMS), if for any solution $e(k)$ with initial state $e(0)$,

$$
\mathscr{E}\left\{\|e(k)\|^2\right\}\le\alpha\|e(0)\|^2\beta^k+\gamma(k),\lim_{k\longrightarrow\infty}\gamma(k)=\bar{\gamma},\tag{13}
$$

holds, where $\alpha>0$, $\beta\in[0,1)$, and $\bar{\gamma}>0$ imply the mean square asymptotic upper bound of (11).

Lemma 1 (see [23]). *Combined with Assumption 1, the nonlinear functions* $\mathbf{f}(e_s(k))$ *and* $\mathbf{h}(e_s(k))$ *of estimation error dynamics (7) satisfy the conditions as follows:*

$$
\begin{aligned}
&\left[e^{\top}(k)\ \ \mathbf{f}^{\top}(e_s(k))\right]\begin{bmatrix}F_1 & *\\ F_2 & I_{Nn_{x_s}}\end{bmatrix}\begin{bmatrix}e(k)\\ \mathbf{f}(e_s(k))\end{bmatrix}\le 0,\\
&\left[e^{\top}(k)\ \ \mathbf{h}^{\top}(e_s(k))\right]\begin{bmatrix}H_1 & *\\ H_2 & I_{Nn_{x_f}}\end{bmatrix}\begin{bmatrix}e(k)\\ \mathbf{h}(e_s(k))\end{bmatrix}\le 0,
\end{aligned}
\tag{14}
$$

where

$$
\begin{aligned}
F_1 &= \operatorname{diag}\left\{I_N\otimes\left(\frac{\Lambda_1^{\top}\Lambda_2+\Lambda_2^{\top}\Lambda_1}{2}\right),0_{Nn_{x_f}}\right\},\\
F_2 &= \left[-I_N\otimes\left(\frac{\Lambda_1+\Lambda_2}{2}\right)\ \ 0_{Nn_{x_s}}\right],\\
H_1 &= \operatorname{diag}\left\{I_N\otimes\left(\frac{\Upsilon_1^{\top}\Upsilon_2+\Upsilon_2^{\top}\Upsilon_1}{2}\right),0_{Nn_{x_f}}\right\},\\
H_2 &= \left[-I_N\otimes\left(\frac{\Upsilon_1+\Upsilon_2}{2}\right)\ \ 0_{Nn_{x_f}}\right].
\end{aligned}
\tag{15}
$$

Lemma 2 (see [23]). *For any matrices* $\mathscr{H}$ *and* $\mathscr{G}$ *and a scalar* $\epsilon_0>0$, $\forall\epsilon\in(0,\epsilon_0]$, *if* $\mathscr{H}\le 0$ *and* $\mathscr{H}+\epsilon_0\mathscr{G}<0$ *hold, it yields* $\mathscr{H}+\epsilon<0$.

3. Main Results

In this section, a sufficient condition is presented to guarantee that the estimation error dynamics (7) is exponentially ultimately bounded in mean square and the desired state estimator will be designed.

Theorem 1. *For given $\epsilon > 0$ and $c \in [0,1)$, estimation error dynamics (7) is EUBMS, if there exist scalars $\lambda_\varsigma > 0\,(\varsigma = 1,2,3)$ and $\kappa > 0$ and matrices $P_\epsilon > 0$, such that*

$$\begin{bmatrix} -(1-c)P_\epsilon - \lambda_1 F_1 - \lambda_2 H_1 & * & * & * & * \\ -\lambda_1 F_2 & -\lambda_1 I_{Nn_{x_s}} & * & * & * \\ -\lambda_2 H_2 & 0 & -\lambda_2 I_{Nn_{x_f}} & * & * \\ 0 & 0 & 0 & -\lambda_3 \Phi & * \\ \sqrt{1+\kappa}\mathscr{A}_\epsilon & \sqrt{1+\kappa}\mathscr{I}_1 & \sqrt{1+\kappa}\epsilon\mathscr{I}_2 & \sqrt{1+\kappa}\mathscr{K} & -P_\epsilon^{-1} \end{bmatrix} < 0, \tag{16}$$

where

$$\Phi = \operatorname{diag}\left\{\Phi_{1s}, \Phi_{2s}, \ldots, \Phi_{Ns}, \Phi_{1f}, \Phi_{2f}, \ldots, \Phi_{Nf}\right\}. \tag{17}$$

Proof. Firstly, construct the following Lyapunov functional candidate:

$$V(k) = e^\top(k) P_\epsilon e(k). \tag{18}$$

According to (5), another equivalent form of the event-triggering condition is as follows:

$$\sum_{i=1}^{N} \theta_i - \bar{\varepsilon}^\top(k)\Phi\bar{\varepsilon}(k) \geq 0. \tag{19}$$

Along the trajectory of (11), calculating the mathematical expectation of the difference of $V(k)$, one gains that

$$\begin{aligned}
\mathscr{E}\{\Delta V(k)\} &= \mathscr{E}\{V(k+1) - (1-c)V(k) - cV(k)\} \\
&= \mathscr{E}\{e^\top(k+1)P_\epsilon e(k+1) - (1-c)e^\top(k)P_\epsilon e(k) - cV(k)\} \\
&\leq \mathscr{E}\{e^\top(k+1)P_\epsilon e(k+1) - (1-c)e^\top(k)P_\epsilon e(k) - cV(k)\} \\
&= \mathscr{E}\Big\{\big(\mathscr{A}_\epsilon e(k) + \mathscr{I}_1\mathbf{f}(e_s(k)) + \epsilon\mathscr{I}_2\mathbf{h}(e_s(k)) + \mathscr{C}_\epsilon \nu(k) + \mathscr{K}\bar{\varepsilon}(k)\big)^\top P_\epsilon \big(\mathscr{A}_\epsilon e(k) + \mathscr{I}_1\mathbf{f}(e_s(k)) \\
&\quad + \epsilon\mathscr{I}_2\mathbf{h}(e_s(k)) + \mathscr{C}_\epsilon \nu(k) + \mathscr{K}\bar{\varepsilon}(k)\big) - (1-c)e^\top(k)P_\epsilon e(k) - cV(k)\Big\} \\
&\leq \mathscr{E}\Big\{\big(\mathscr{A}_\epsilon e(k) + \mathscr{I}_1\mathbf{f}(e_s(k)) + \epsilon\mathscr{I}_2\mathbf{h}(e_s(k)) + \mathscr{K}\bar{\varepsilon}(k)\big)^\top P_\epsilon \big(\mathscr{A}_\epsilon e(k) + \mathscr{I}_1\mathbf{f}(e_s(k))\big) + \epsilon\mathscr{I}_2\mathbf{h}(e_s(k)) \\
&\quad + \mathscr{K}\bar{\varepsilon}(k)\big) + \nu^\top(k)\mathscr{C}_\epsilon^\top P_\epsilon \mathscr{C}_\epsilon \nu(k) + 2\big(\mathscr{A}_\epsilon e(k) + \mathscr{I}_1\mathbf{f}(e_s(k))\big) + \epsilon\mathscr{I}_2\mathbf{h}(e_s(k)) + \mathscr{K}\bar{\varepsilon}(k)\big)^\top P_\epsilon \mathscr{C}_\epsilon \nu(k) \\
&\quad - (1-c)e^\top(k)P_\epsilon e(k) - cV(k)\Big\}.
\end{aligned} \tag{20}$$

Depending on Young's inequality, the following inequality holds:

$$\begin{aligned}
&2\big(\mathscr{A}_\epsilon e(k) + \mathscr{I}_1\mathbf{f}(e_s(k)) + \epsilon\mathscr{I}_2\mathbf{h}(e_s(k)) + \mathscr{K}\bar{\varepsilon}(k)\big)^\top P_\epsilon \mathscr{C}_\epsilon \nu(k) \\
&\quad \leq \kappa\big(\mathscr{A}_\epsilon e(k) + \mathscr{I}_1\mathbf{f}(e_s(k)) + \epsilon\mathscr{I}_2\mathbf{h}(e_s(k)) + \mathscr{K}\bar{\varepsilon}(k)\big)^\top P_\epsilon \big(\mathscr{A}_\epsilon e(k) + \mathscr{I}_1\mathbf{f}(e_s(k)) + \epsilon\mathscr{I}_2\mathbf{h}(e_s(k)) + \mathscr{K}\bar{\varepsilon}(k)\big)\big) \\
&\quad\quad + \frac{1}{\kappa}\big(\nu^\top(k)\mathscr{C}_\epsilon^\top P_\epsilon \mathscr{C}_\epsilon \nu(k)\big).
\end{aligned} \tag{21}$$

Combining (19) and (21) and Lemma 1, we obtain that

$$\mathscr{E}\{\Delta V(k)\} \leq \mathscr{E}\left\{\begin{array}{c}(1+\kappa)\left(\mathscr{A}_\epsilon e(k)+\mathscr{I}_1\mathbf{f}(e_s(k))+\epsilon\mathscr{I}_2\mathbf{h}(e_s(k))+\mathscr{K}\bar{\varepsilon}(k)\right)^\top P_\epsilon\left(\mathscr{A}_\epsilon e(k)+\mathscr{I}_1\mathbf{f}(e_s(k))+\epsilon\mathscr{I}_2\mathbf{h}(e_s(k))+\mathscr{K}\bar{\varepsilon}(k)\right) \\ +\left(1+\dfrac{1}{\kappa}\right)\nu^\top(k)\mathscr{C}_\epsilon^\top P_\epsilon\mathscr{C}_\epsilon\nu(k)-(1-c)e^\top(k)P_\epsilon e(k)-cV(k)-\lambda_1\left(\begin{bmatrix}e^\top(k) & \mathbf{f}^\top(e_s(k))\end{bmatrix}\begin{bmatrix}F_1 & * \\ F_2 & I_{Nn_{x_s}}\end{bmatrix}\begin{bmatrix}e(k) \\ \mathbf{f}(e_s(k))\end{bmatrix}\right) \\ -\lambda_2\left(\begin{bmatrix}e^\top(k) & \mathbf{h}^\top(e_s(k))\end{bmatrix}\begin{bmatrix}H_1 & * \\ H_2 & I_{Nn_{x_f}}\end{bmatrix}\begin{bmatrix}e(k) \\ \mathbf{h}(e_s(k))\end{bmatrix}\right)+\lambda_3\left(\sum_{i=1}^N\theta_i-\bar{\varepsilon}^\top(k)\Phi\bar{\varepsilon}(k)\right)\end{array}\right\} \tag{22}$$

$$= \aleph^\top(k)\Xi_\epsilon\aleph(k)-cV(k)+\varrho,$$

where

$$\aleph(k) = \left[e^\top(k)\mathbf{f}^\top(e_s(k))\mathbf{h}^\top(e_s(k))\bar{\varepsilon}^\top(k)\right]^\top,$$

$$\varrho = \lambda_3\sum_{i=1}^N\theta_i+\left(1+\frac{1}{\kappa}\right)\lambda_{\max}\{\mathscr{C}_\epsilon^\top P_\epsilon\mathscr{C}_\epsilon\}\bar{\nu},$$

$$\Xi_\epsilon = \begin{bmatrix}\Xi_\epsilon^{11} & * & * & * \\ (1+\kappa)\mathscr{I}_1^\top P_\epsilon\mathscr{A}_\epsilon-\lambda_1F_2 & (1+\kappa)\mathscr{I}_1^\top P_\epsilon\mathscr{I}_1-\lambda_1I_{Nn_{x_s}} & * & * \\ (1+\kappa)\epsilon\mathscr{I}_2^\top P_\epsilon\mathscr{A}_\epsilon-\lambda_2H_2 & (1+\kappa)\epsilon\mathscr{I}_2^\top P_\epsilon\mathscr{I}_1 & (1+\kappa)\epsilon^2\mathscr{I}_2^\top P_\epsilon\mathscr{I}_2-\lambda_2I_{Nn_{x_f}} & * \\ (1+\kappa)\mathscr{K}^\top P_\epsilon\mathscr{A}_\epsilon & (1+\kappa)\mathscr{K}^\top P_\epsilon\mathscr{I}_1 & (1+\kappa)\mathscr{K}^\top P_\epsilon\epsilon\mathscr{I}_2 & (1+\kappa)\mathscr{K}^\top P_\epsilon\mathscr{K}-\lambda_3\Phi\end{bmatrix}, \tag{23}$$

$$\Xi_\epsilon^{11} = (1+\kappa)\mathscr{A}_\epsilon^\top P_\epsilon\mathscr{A}_\epsilon-(1-c)P_\epsilon-\lambda_1F_1-\lambda_2H_1.$$

Applying the Schur complement lemma to (16), it is clear that $\Xi_\epsilon < 0$. Consequently, one has

$$\mathscr{E}\{\Delta V(k)\} \leq -cV(k)+\varrho, \tag{24}$$

which yields

$$\mathscr{E}\{V(k+1)\} \leq (1-c)V(k)+\varrho. \tag{25}$$

Then, it follows from (25) that

$$\mathscr{E}\{V(k)\} \leq (1-c)^kV(0)+\frac{1-(1-c)^k}{c}\varrho. \tag{26}$$

Moreover, it is easy to obtain that $V(k) \geq \lambda_{\min}\{P_\epsilon\}e^\top(k)e(k)$ and $V(0) \leq \lambda_{\max}\{P_\epsilon\}e^\top(0)e(0)$; combining (26), it yields that

$$\mathscr{E}\left\{\|e(k)\|^2\right\} \leq \frac{(1-c)^k\lambda_{\max}\{P_\epsilon\}}{\lambda_{\min}\{P_\epsilon\}}\|e(0)\|^2+\frac{1-(1-c)^k}{c\lambda_{\min}\{P_\epsilon\}}\varrho. \tag{27}$$

Consequently, estimation error dynamics (7) is EUBMS, and $\bar{\gamma} = 1/c\lambda_{\min}\{P_\epsilon\}\varrho$ is the mean square asymptotic upper bound of (7), which completes the proof. □

Theorem 2. *For* $\forall\epsilon \in (0,\epsilon_0]$ *with the upper bound* $\epsilon_0 > 0$ *and* $c \in [0,1)$, *estimation error dynamics (7) is EUBMS, if there exist scalars* $\lambda_\varsigma(\varsigma = 1,2,3)$ *and* $\kappa > 0$ *and matrices* $\breve{P} = \begin{bmatrix}\breve{P}_{11} & * \\ \breve{P}_{21} & \breve{P}_{22}\end{bmatrix}$, $\hat{P} = \begin{bmatrix}\hat{P}_{11} & * \\ \hat{P}_{21} & \hat{P}_{22}\end{bmatrix}$, $X_\ell = diag\{X_{\ell1}, X_{\ell2}, \ldots, X_{\ell N}\}$ $(\ell = 1,2)$, *and* $\overline{K}_{i\wp}(i = 1,2,\ldots,N, \wp = s,f)$, *such that*

$$\breve{P} \geq 0, \breve{P} + \epsilon_0 \widehat{P} > 0, \tag{28}$$

$$\begin{bmatrix} -(1-c)\breve{P} - \lambda_1 F_1 - \lambda_2 H_1 & * & * & * & * \\ -\lambda_1 F_2 & -\lambda_1 I_{Nn_{x_s}} & * & * & * \\ -\lambda_2 H_2 & 0 & -\lambda_2 I_{Nn_{x_f}} & * & * \\ 0 & 0 & 0 & -\lambda_3 \Phi & * \\ \sqrt{1+\kappa}\,\breve{\mathscr{A}} & \sqrt{1+\kappa}\,X\mathscr{I}_1 & 0 & \sqrt{1+\kappa}\,\widetilde{\mathscr{K}} & \breve{P} - X - X^\top \end{bmatrix} \leq 0, \tag{29}$$

$$\begin{bmatrix} -(1-c)\left(\breve{P} + \epsilon_0\widehat{P}\right) - \lambda_1 F_1 - \lambda_2 H_1 & * & * & * & * \\ -\lambda_1 F_2 & -\lambda_1 I_{Nn_{x_s}} & * & * & * \\ -\lambda_2 H_2 & 0 & -\lambda_2 I_{Nn_{x_f}} & * & * \\ 0 & 0 & 0 & -\lambda_3 \Phi & * \\ \sqrt{1+\kappa}\left(\breve{\mathscr{A}} + \epsilon_0\widehat{\mathscr{A}}\right) & \sqrt{1+\kappa}\,X\mathscr{I}_1 & \sqrt{1+\kappa}\,\epsilon_0 X\mathscr{I}_2 & \sqrt{1+\kappa}\,\widetilde{\mathscr{K}} & \breve{P} + \epsilon_0\widehat{P} - X - X^\top \end{bmatrix} < 0, \tag{30}$$

where

$$\begin{aligned} X &= \mathrm{diag}\{X_1, X_2\}, \\ \overline{K}_\wp &= \mathrm{diag}\left\{\overline{K}_{1\wp}, \overline{K}_{2\wp}, \ldots, \overline{K}_{N\wp}\right\}, (\wp = s, f), \\ \breve{\mathscr{A}} &= \begin{bmatrix} -\overline{K}_s D_s + X_1(\mathscr{W} \otimes \Gamma_{11}) & X_1(I_N \otimes A + \mathscr{W} \otimes \Gamma_{12}) \\ 0 & -\overline{K}_f D_f \end{bmatrix}, \\ \widehat{\mathscr{A}} &= \begin{bmatrix} 0 & 0 \\ X_2(\mathscr{W} \otimes \Gamma_{21}) & X_2(I_N \otimes B + \mathscr{W} \otimes \Gamma_{22}) \end{bmatrix}, \\ \widetilde{\mathscr{K}} &= \mathrm{diag}\left\{\overline{K}_s, \overline{K}_f\right\}. \end{aligned} \tag{31}$$

Moreover, the estimator gain matrices are calculated as

$$\begin{aligned} K_{is} &= X_{1i}^{-1}\overline{K}_{is}, \\ K_{if} &= X_{2i}^{-1}\overline{K}_{if}, \\ &(i = 1, 2, \ldots, N). \end{aligned} \tag{32}$$

Proof. From (28)–(30) and Lemma 2, it follows that for $\forall\epsilon \in (0, \epsilon_0]$, the following conditions hold:

$$P_\epsilon = \breve{P} + \epsilon\widehat{P} > 0$$

$$\cdot \begin{bmatrix} -(1-c)(\breve{P} + \epsilon\widehat{P}) - \lambda_1 F_1 - \lambda_2 H_1 & * & * & * & * \\ -\lambda_1 F_2 & -\lambda_1 I_{Nn_{x_s}} & * & * & * \\ -\lambda_2 H_2 & 0 & -\lambda_2 I_{Nn_{x_f}} & * & * \\ 0 & 0 & 0 & -\lambda_3 \Phi & * \\ \sqrt{1+\kappa}\,(\breve{\mathscr{A}} + \epsilon\widehat{\mathscr{A}}) & \sqrt{1+\kappa}\,X\mathscr{I}_1 & \sqrt{1+\kappa}\,\epsilon X\mathscr{I}_2 & \sqrt{1+\kappa}\,\widetilde{\mathscr{K}} & \breve{P} + \epsilon\widehat{P} - X - X^\top \end{bmatrix} < 0. \tag{33}$$

Substituting (32) into (33) and noticing that $-XP_\epsilon^{-1}X^\top \leq P_\epsilon - \mathbf{He}\{X\}$, one has

$$\begin{bmatrix} -(1-c)P_\epsilon - \lambda_1 F_1 - \lambda_2 H_1 & * & * & * & * \\ -\lambda_1 F_2 & -\lambda_1 I_{Nn_{x_s}} & * & * & * \\ -\lambda_2 H_2 & 0 & -\lambda_2 I_{Nn_{x_f}} & * & * \\ 0 & 0 & 0 & -\lambda_3 \Phi & * \\ \sqrt{1+\kappa}\,X\mathscr{A}_\epsilon & \sqrt{1+\kappa}\,X\mathscr{I}_1 & \sqrt{1+\kappa}\,\epsilon X\mathscr{I}_2 & \sqrt{1+\kappa}\,X\mathscr{K} & -XP_\epsilon^{-1}X^\top \end{bmatrix} < 0. \tag{34}$$

Recalling (29), it is clear that $\breve{P} - X - X^\top < 0$ with $\breve{P} \geq 0$. Then, X is invertible.

Premultiplying and postmultiplying (34) by $\text{diag}\{I_{Nn_x}, I_{Nn_{x_s}}, I_{2Nn_{x_f}}, I_{Nn_y}, X^{-1}\}$, its transposes yields (16). Therefore, inequality (16) can be guaranteed if (28)–(30) hold. This completes the proof. □

4. Numerical Example

Similar to [23], consider SPCNs (1) with three nodes and the following parameters:

$$\begin{aligned}
A &= \begin{bmatrix} 1.2 & 0.45 \end{bmatrix}, \\
B &= \begin{bmatrix} 1.3 & 0.6 \\ 2.3 & 0.9 \end{bmatrix}, \\
C_{1s} &= 0.2, \\
C_{2s} &= 0.1, \\
C_{3s} &= 0.4, \\
C_{1f} &= \begin{bmatrix} 0.86 \\ 1.15 \end{bmatrix}, \\
C_{2f} &= \begin{bmatrix} 0.5 \\ 1.75 \end{bmatrix}, \\
C_{3f} &= \begin{bmatrix} 0.02 \\ 0.05 \end{bmatrix}, \\
D_{1s} &= \begin{bmatrix} 2 \\ 1.2 \end{bmatrix}, \\
D_{2s} &= \begin{bmatrix} 0.9 \\ 2.1 \end{bmatrix}, \\
D_{3s} &= \begin{bmatrix} 1.6 \\ 1.62 \end{bmatrix}, \\
D_{1f} &= \begin{bmatrix} 2.4 & 1 \end{bmatrix}, \\
D_{2f} &= \begin{bmatrix} -1.4 & 0.6 \end{bmatrix}, \\
D_{3f} &= \begin{bmatrix} 2.3 & 2 \end{bmatrix}, \\
E_{1s} &= \begin{bmatrix} 0.8 \\ 1 \end{bmatrix}, \\
E_{2s} &= \begin{bmatrix} 0.5 \\ 0.1 \end{bmatrix}, \\
E_{3s} &= \begin{bmatrix} 0.4 \\ -1 \end{bmatrix}, \\
E_{1f} &= 0.2, \\
E_{1f} &= 0.4, \\
E_{1f} &= 0.25.
\end{aligned} \tag{35}$$

The out-coupled configuration matrix $\mathscr{W}$ of SPCNs (1) and its inner-coupling matrix, respectively, are selected as follows:

$$\begin{aligned}
\Gamma_{11} &= 0.45, \\
\Gamma_{12} &= \begin{bmatrix} 0.2 & 0.6 \end{bmatrix}, \\
\Gamma_{21} &= \begin{bmatrix} 0.1 \\ 0.5 \end{bmatrix}, \\
\Gamma_{22} &= \begin{bmatrix} 0.6 & 0.2 \\ 0.4 & 0.25 \end{bmatrix}, \\
\mathscr{W} &= \begin{bmatrix} -0.2 & 0.1 & 0.1 \\ 0.1 & -0.2 & 0.1 \\ 0.1 & 0.1 & -0.2 \end{bmatrix}.
\end{aligned} \tag{36}$$

In light of Assumption 1, the nonlinear vector-valued functions are chosen as

$$\begin{aligned}
f(x_{is}(k)) &= 0.8x_{is}(k) - \tanh(0.4x_{is}(k)), \\
h(x_{is}(k)) &= \begin{bmatrix} 0.3x_{is}(k) - \tanh(0.1x_{is}(k)) \\ 0.4x_{is}(k) - \tanh(0.2x_{is}(k)) \end{bmatrix}, \quad (i = 1, 2, \ldots, N),
\end{aligned} \tag{37}$$

and $\Lambda_1 = 0.5, \Lambda_2 = 0.58, \Upsilon_1 = \begin{bmatrix} 0.2 & 0.2 \end{bmatrix}^\top$, and $\Upsilon_2 = \begin{bmatrix} 0.5 & 0.41 \end{bmatrix}^\top$. The event-triggered thresholds are set as $\theta_1 = 0.17$, $\theta_2 = 0.104$, and $\theta_3 = 0.5$, and the weighting matrices are calculated as $\Phi_i = \text{diag}\{44.1124, 44.1124, 44.1124\}$ $(i = 1, 2, 3)$. Other parameters are given as follows: $\epsilon_0 = 0.0193$ and $c = 0.1$.

According to Theorem 2, the gain matrices of state estimator (6) can be obtained as

$$\begin{aligned}
K_s &= \begin{bmatrix} 0.1755 & 0.1053 & 0 & 0 & 0 & 0 \\ 0 & 0 & 0.0824 & 0.1924 & 0 & 0 \\ 0 & 0 & 0 & 0 & 0.1473 & 0.1491 \end{bmatrix}, \\
K_f &= \begin{bmatrix} 0.0107 & 0 & 0 \\ 0.0290 & 0 & 0 \\ 0 & -0.0179 & 0 \\ 0 & -0.1104 & 0 \\ 0 & 0 & 0.0102 \\ 0 & 0 & 0.0222 \end{bmatrix}.
\end{aligned} \tag{38}$$

The bound disturbance input is considered as $\nu(k) = 0.05\cos(2k)$, and the initial conditions of (1) and (6) are given as $x_1(0) = \begin{bmatrix} 0.04 & 0.01 & 0.02 \end{bmatrix}^\top$, $x_2(0) = \begin{bmatrix} 0.03 & 0.015 & 0.02 \end{bmatrix}^\top$, $x_3(0) = \begin{bmatrix} 0.1 & 0.004 & 0.004 \end{bmatrix}^\top$, and $\widehat{x}_1(0) = \widehat{x}_2(0) = \widehat{x}_3(0) = \begin{bmatrix} 0 & 0 & 0 \end{bmatrix}^\top$.

The simulation results are presented in Figures 1–5. Figures 1–3 display the state trajectories and their estimations of three nodes, respectively. The event-based release instants and release intervals of three nodes are shown in Figure 4. Figure 5 plots the evolutions of the estimation error dynamics. It can be discovered from Figure 5 that estimation error dynamics (7) is EUBMS.

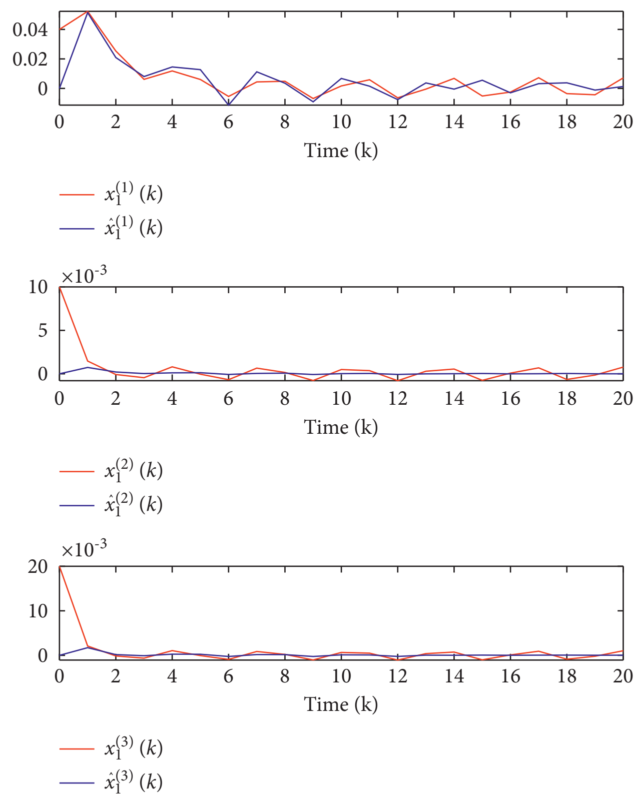

Figure 1: The state trajectories and estimations of node 1.

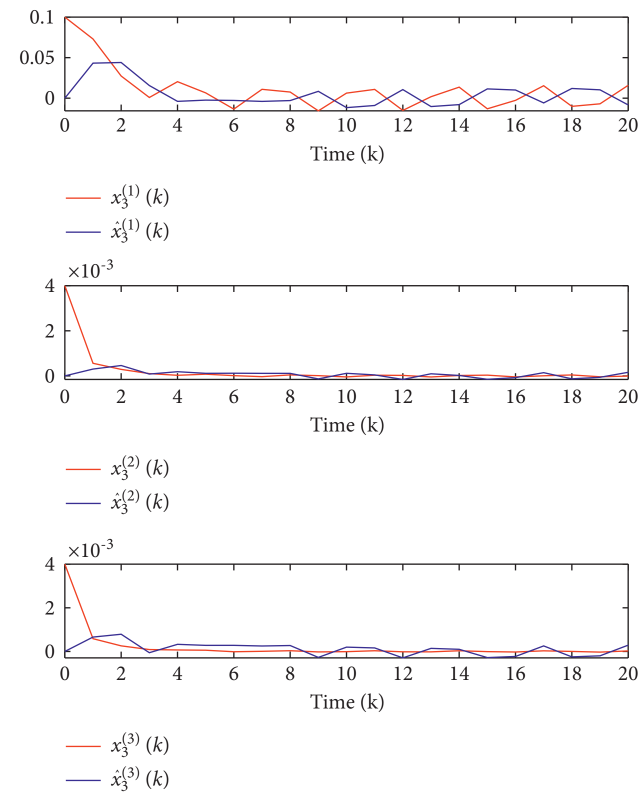

Figure 3: The state trajectories and estimations of node 3.

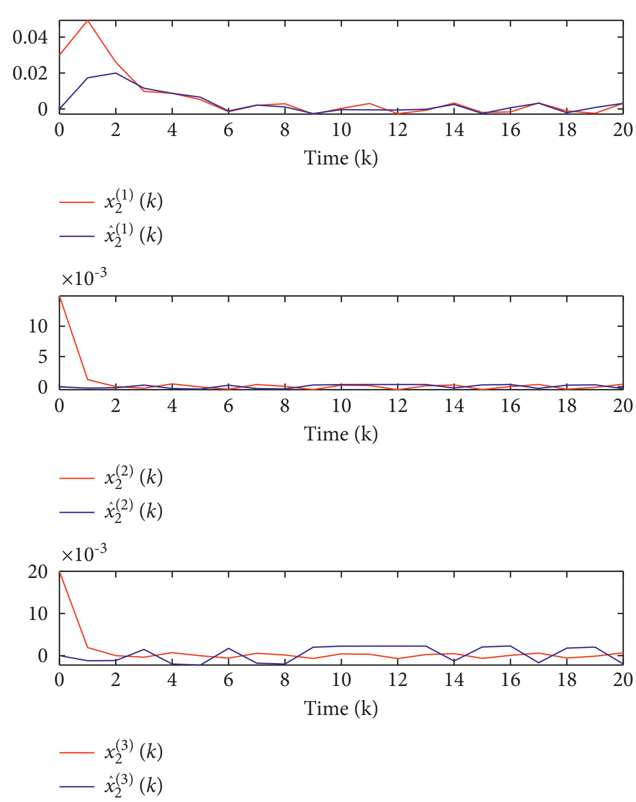

Figure 2: The state trajectories and estimations of node 2.

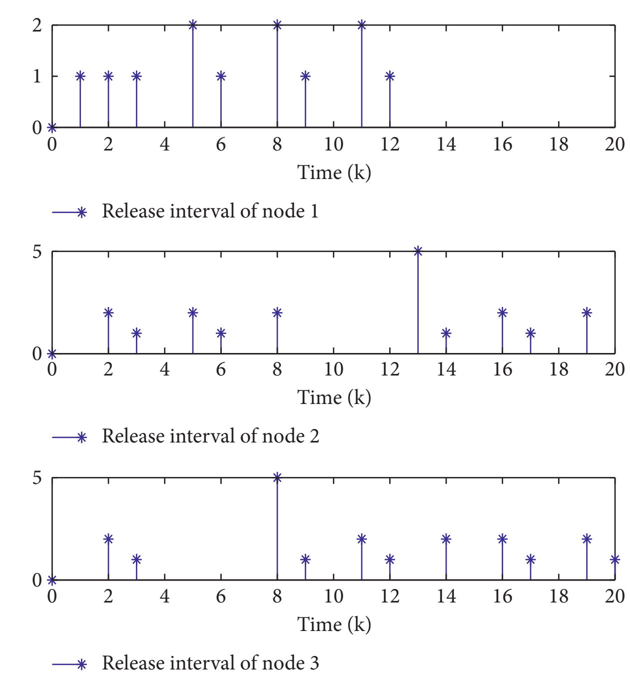

Figure 4: The event-based release instants and release intervals of three nodes.

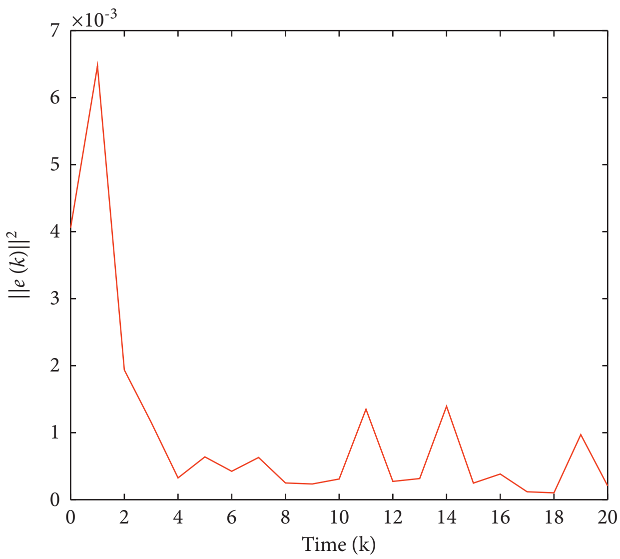

Figure 5: Dynamics of the estimation error $e(k)$.

5. Conclusions

This paper has investigated the issue of the multievent-triggered state estimation for a novel class of discrete-time nonlinear SPCNs. A discrete-time SPCN model with nonlinearities has been modeled. To alleviate energy consumption, a multievent triggered protocol is applied to regulate the communication among nodes of the SPCNs. Finally, a simulation has demonstrated the rationality, superiority, and effectiveness of the proposed method.

Data Availability

The data used to support the findings of this study are available from the author upon request.

Conflicts of Interest

The author declares no conflicts of interest.

Acknowledgments

This work was supported by the Project of Youth Science and Technology Talents of Guizhou Province (Grant Number: Qian Jiao He KY Zi[2020]095).

References

[1] J. M. Carrasco, L. G. Franquelo, J. T. Bialasiewicz et al., "Power-electronic systems for the grid integration of renewable energy sources: a survey," *IEEE Transactions on Industrial Electronics*, vol. 53, no. 4, pp. 1002–1016, 2006.

[2] G. Feng, J. Cao, and J. Lu, "Impulsive synchronization of nonlinearly coupled complex networks," *Mathematical Problems in Engineering*, vol. 2012, Article ID 969402, 11 pages, 2012.

[3] Y. Chen, D. Zhang, H. Zhang, and Q.-G. Wang, "Dual-path mixed domain residual threshold networks for bearing fault diagnosis," *IEEE Transactions on Industrial Electronics*, p. 1, 2022.

[4] K. Musial, P. Bródka, and P. De Meo, "Analysis and Applications of Complex Social Networks," *Complexity*, vol. 2017, Article ID 3014163, 17 pages, 2017.

[5] X. Wu, J. Feng, and Z. Nie, "Outer synchronization of drive-response complex-valued complex networks via intermittent pinning control," *Complexity*, vol. 2021, Article ID 6649519, 10 pages, 2021.

[6] Z.-G. Wu, Z. Xu, P. Shi, M. Z. Chen, and H. Su, "Nonfragile state estimation of quantized complex networks with switching topologies," *IEEE Transactions on Neural Networks and Learning Systems*, vol. 29, no. 10, pp. 5111–5121, 2018.

[7] W. Qi, G. Zong, and C. K. Ahn, "Input-output finite-time asynchronous smc for nonlinear semi-markov switching systems with application," *IEEE Transactions on Systems, Man, and Cybernetics: Systems*, pp. 1–10, 2021.

[8] S. Fan, H. Yan, H. Zhang, H. Shen, and K. Shi, "Dynamic event-based non-fragile dissipative state estimation for quantized complex networks with fading measurements and its application," *IEEE Transactions on Circuits and Systems I: Regular Papers*, vol. 68, no. 2, pp. 856–867, 2020.

[9] S. Wang, Z. Wang, H. Dong, and Y. Chen, "A dynamic event-triggered approach to recursive nonfragile filtering for complex networks with sensor saturations and switching topologies," *IEEE Transactions on Cybernetics*, pp. 1–14, 2021.

[10] P. Kokotović, H. K. Khalil, and J. O'reilly, *Singular Perturbation Methods in Control: Analysis and Design*, Academic Press Inc, Cambridge, MA, USA, 1999.

[11] J. R. Winkelman, J. H. Chow, J. J. Allemong, and P. V. Kokotovic, "Multi-time-scale analysis of a power system," *Automatica*, vol. 16, no. 1, pp. 35–43, 1980.

[12] R. Wang, T. Chen, Z. Zhou, and L. Jing, "Modelling periodic oscillation of biological systems with multiple timescale networks," *Systematic Biology*, vol. 1, no. 1, pp. 71–84, 2004.

[13] J. Cheng, J. H. Park, Z.-G. Wu, and H. Yan, "Ultimate boundedness control for networked singularly perturbed systems with deception attacks: a Markovian communication protocol approach," *IEEE Transactions on Network Science and Engineering*, vol. 9, no. 2, pp. 445–456, 2021.

[14] J. Cheng, W. Huang, H.-K. Lam, J. Cao, and Y. Zhang, "Fuzzy-model-based control for singularly perturbed systems with nonhomogeneous Markov switching: a dropout compensation strategy," *IEEE Transactions on Fuzzy Systems*, vol. 30, no. 2, pp. 530–541, 2022.

[15] J. Cheng, Y. Wang, J. H. Park, J. Cao, and K. Shi, "Static output feedback quantized control for fuzzy Markovian switching singularly perturbed systems with deception attacks," *IEEE Transactions on Fuzzy Systems*, vol. 30, no. 4, pp. 1036–1047, 2022.

[16] P. Zeng and Z. Zeng, "Synchronization of delayed complex networks on time scales via aperiodically intermittent control using matrix-based convex combination method," *IEEE Transactions on Neural Networks and Learning Systems*, pp. 1–13, 2021.

[17] K. Sivaranjani, R. Rakkiyappan, J. Cao, and A. Alsaedi, "Synchronization of nonlinear singularly perturbed complex networks with uncertain inner coupling via event triggered control," *Applied Mathematics and Computation*, vol. 311, pp. 283–299, 2017.

[18] W.-H. Chen, Y. Liu, and W. X. Zheng, "Synchronization analysis of two-time-scale nonlinear complex networks with time-scale-dependent coupling," *IEEE Transactions on Cybernetics*, vol. 49, no. 9, pp. 3255–3267, 2018.

[19] K. Liang, W. He, J. Xu, and F. Qian, "Impulsive effects on synchronization of singularly perturbed complex networks with semi-markov jump topologies," *IEEE Transactions on Systems, Man, and Cybernetics: Systems*, vol. 52, no. 5, pp. 3163–3173, 2022.
[20] S. Yang and X.-S. Yang, "Bounded synchronisation of singularly perturbed complex network with an application to power systems," *IET Control Theory & Applications*, vol. 8, no. 1, pp. 61–66, 2014.
[21] C. Cai, Z. Wang, J. Xu, X. Liu, and F. E. Alsaadi, "An integrated approach to global synchronization and state estimation for nonlinear singularly perturbed complex networks," *IEEE Transactions on Cybernetics*, vol. 45, no. 8, pp. 1597–1609, 2014.
[22] X. Wan, Z. Wang, M. Wu, and X. Liu, "State estimation for discrete-time nonlinear singularly perturbed complex networks under the round-robin protocol," *IEEE Transactions on Neural Networks and Learning Systems*, vol. 30, no. 2, pp. 415–426, 2018.
[23] X. Wan, Y. Li, Y. Li, and M. Wu, "Finite-time H ∞ state estimation for two-time-scale complex networks under stochastic communication protocol," *IEEE Transactions on Neural Networks and Learning Systems*, vol. 33, no. 1, pp. 25–36, 2022.
[24] N. Hou, H. Dong, W. Zhang, Y. Liu, and F. E. Alsaadi, "Event-triggered state estimation for time-delayed complex networks with gain variations based on partial nodes," *International Journal of General Systems*, vol. 47, no. 5, pp. 477–490, 2018.
[25] L. Wang, Z. Wang, T. Huang, and G. Wei, "An event-triggered approach to state estimation for a class of complex networks with mixed time delays and nonlinearities," *IEEE Transactions on Cybernetics*, vol. 46, no. 11, pp. 2497–2508, 2015.
[26] Y. Liu, Z. Wang, Y. Yuan, and W. Liu, "Event-triggered partial-nodes-based state estimation for delayed complex networks with bounded distributed delays," *IEEE Transactions on Systems, Man, and Cybernetics: Systems*, vol. 49, no. 6, pp. 1088–1098, 2017.
[27] Z. Yan, X. Huang, Y. Fan, J. Xia, and H. Shen, "Threshold-function-dependent quasi-synchronization of delayed memristive neural networks via hybrid event-triggered control," *IEEE Transactions on Systems, Man, and Cybernetics: Systems*, vol. 51, no. 11, pp. 6712–6722, 2020.
[28] J. Cheng, L. Liang, J. H. Park, H. Yan, and K. Li, "A dynamic event-triggered approach to state estimation for switched memristive neural networks with nonhomogeneous sojourn probabilities," *IEEE Transactions on Circuits and Systems I: Regular Papers*, vol. 68, no. 12, pp. 4924–4934, 2021.
[29] Y. Fan, X. Huang, Z. Wang, J. Xia, and H. Shen, "Discontinuous event-triggered control for local stabilization of memristive neural networks with actuator saturation: discrete- and continuous-time lyapunov methods," *IEEE Transactions on Neural Networks and Learning Systems*, pp. 1–13, 2021.
[30] Z. Ye, D. Zhang, Z.-G. Wu, and H. Yan, "A3C-based intelligent event-triggering control of networked nonlinear unmanned marine vehicles subject to hybrid attacks," *IEEE Transactions on Intelligent Transportation Systems*, pp. 1–14, 2021.
[31] L. Xie, J. Cheng, H. Wang, J. Wang, M. Hu, and Z. Zhou, "Memory-based event-triggered asynchronous control for semi-markov switching systems," *Applied Mathematics and Computation*, vol. 415, Article ID 126694, 2022.
[32] S. Zhu, E. Tian, D. Xu, and J. Liu, "An adaptive torus-event-based controller design for networked T-S fuzzy systems under deception attacks," *International Journal of Robust and Nonlinear Control*, vol. 32, no. 6, pp. 3425–3441, 2022.
[33] F. Qu, X. Zhao, X. Wang, and E. Tian, "Probabilistic-constrained distributed fusion filtering for a class of time-varying systems over sensor networks: a torus-event-triggering mechanism," *International Journal of Systems Science*, vol. 53, no. 6, pp. 1288–1297, 2022.
[34] J. Cheng, Y. Wu, H. Yan, Z.-G. Wu, and K. Shi, "Protocol-based filtering for fuzzy Markov affine systems with switching chain," *Automatica*, vol. 141, Article ID 110321, 2022.
[35] D. Zhao, Z. Wang, D. W. Ho, and G. Wei, "Observer-based pid security control for discrete time-delay systems under cyber-attacks," *IEEE Transactions on Systems, Man, and Cybernetics: Systems*, vol. 51, no. 6, pp. 3926–3938, 2019.